

# Theoretical analysis of the secondary development of mining-induced surface cracks in the Ordos region

Yuankun Xu<sup>1</sup> · Kan Wu<sup>1</sup> · Zhihui Bai<sup>2</sup> · Zhenqi Hu<sup>3</sup>

Received: 24 February 2017 / Accepted: 11 October 2017 / Published online: 19 October 2017  
© Springer-Verlag GmbH Germany 2017

**Abstract** Prior studies have indicated that mining-induced surface dynamic cracks in eastern China only undergo one “expanding-closure” development cycle. However, field measurements from the Bulianta mines of northwestern China demonstrated that ground dynamic cracks in the Ordos region went through two “expanding-closure” cycle. Using in situ measurement data and theoretical analysis, we find that the strata control theory cannot reasonably explain this special phenomenon. In this paper, we propose a novel explanation from the perspective of soil mechanics. A comparison of two field examples in eastern and northwestern China demonstrates that our theoretical explanation is in agreement with in situ observations and therefore is a reasonable interpretation for the secondary development of ground dynamic cracks in the Bulianta mines. This study provides a theoretical basis for the mechanism of mining-induced ground dynamic cracks.

**Keywords** Coal mining · Ground subsidence · Soil mechanics · Aeolian region

## Introduction

Environmental problems caused by underground coal exploitation, such as ground subsidence, surface cracks, and collapse pit, have long been a research focus (Prakash et al. 2014). Located in a typical windy desert region of western China, the Ordos coalfield is covered by aeolian sand and has sparse vegetation. Because the coal seam thickness exceeds 5 m, intensive excavation brings about significant severe ground subsidence and dense surface cracks (Li et al. 2017). As the surface layer is composed of aeolian sand, the development mechanism for surface cracks is unique.

The mining-induced surface cracks include two types, namely static cracks and dynamic cracks. The static cracks usually have larger width than the dynamic cracks. From the overhead view, the static cracks are located at the margin of the working face, and once formed, they will not close even after the mining activities has ended. Conversely, the dynamic cracks are situated within the scope of the working face, and they would undergo periodic variation of generation, expansion to restoration in the mining process (Li et al. 2017; Dunrud and Osterwald 1980). In this paper, we mainly pay attention to the dynamic cracks.

The development characteristics of surface dynamic cracks induced by underground coal mining have been investigated by many scholars. Yuan and Wu (2003) analyzed the development characteristics of mining-induced surface cracks in eastern China to assess embankment safety. Through in situ measurement of the width and depth, they found that the surface cracks in eastern China

✉ Kan Wu  
wuakan6899@cumt.edu.cn

Yuankun Xu  
xuyuankun@cumt.edu.cn

Zhihui Bai  
531147384@qq.com

Zhenqi Hu  
huzhenqi53@163.com

<sup>1</sup> School of Environment Science and Spatial Informatics, China University of Mining and Technology, Xuzhou 221116, People's Republic of China

<sup>2</sup> Fengfeng Group, Jizhong Energy Group Co., Ltd, Handan 056000, People's Republic of China

<sup>3</sup> Institute of Land Reclamation and Ecological Restoration, China University of Mining and Technology (Beijing), Beijing 100083, People's Republic of China

presented a unimodal “expanding-closure” development cycle. Furthermore, they concluded that surface cracks were caused by ground tensile deformation and cracks started to close almost instantly when the ground evolved into a compression state. However, in northwestern China, Hu et al. (2014) conducted dynamic monitoring of ground fissures at the Bulianta coal mines and found that the width of ground fissures displayed an unusual M-shaped developmental cycle. Similar phenomenon is also valid in other coalfield in various countries (Sirdesai et al. 2015; Verma et al. 2013; Singh and Singh 1992). Wang (2014) attributed this special phenomenon to two hard strata, the key strata, which was partially supported by field observations.

The goal of this study is to interpret the secondary development of surface cracks observed by Hu et al. (2014). A novel hypothesis that uses soil mechanics to explain in situ measurements provides a better explanation for ground cracks with two “expanding-closure” development cycles.

## Materials and methods

### Field measurements of ground settlement and surface cracks

We chose a typical working face of the Bulianta mines in Ordos, China, as the field example to obtain data for ground subsidence and surface cracks caused by underground coal exploitation in an aeolian region. The coal seams of Bulianta mines have an average thickness of 5 m, a burial depth of 190–220 m, and a dip angle of 1°–3°. The typical stratigraphic column of Bulianta mines is shown in Table 1.

As shown in Fig. 1, we set two perpendicular observation lines, 900 and 1100 m long, above the selected working face. The neighboring observation points were 20–30 m distant from each other, and eight control points, K1–K8, were set outside the subsidence area. We adopted second-order leveling<sup>1</sup> to record surface dynamic subsidence, and measurement precision was within 2 mm. A handheld GPS unit and a steel ruler were, respectively, used to record location, width, and length of surface cracks. In addition, some cracks were grouted with the mixture of plaster and water and then excavated to measure the depth.

### Theoretical hypothesis and analysis

The primary reason for the formation of surface cracks lies in the shearing force inside the soil mass due to internal

<sup>1</sup> Specifications for the first-order leveling and second-order leveling in China, GBT12897-2006.

**Table 1** Typical strata structure of Bulianta mines (Xu et al. 2017)

No.	Rock type	Thickness (m)
1	Weathered sandstone	17
2	Glutenite	14.35
3	Medium-grained sandstone	33.07
4	Mudstone and silty mudstone	1.53
5	Medium-grained sandstone	10.19
6	Glutenite	2.42
7	Fine sandstone	4.45
8	Glutenite	16.24
9	Fine sandstone	7.27
10	Sandy mudstone	6.58
11	Mudstone and silty mudstone	3.96
12	Silty mudstone	13.89
13	Silty mudstone	33.2
14	Coarse-grained sandstone	7.62
15	Medium-grained sandstone	3.74
16	Silty mudstone	3.4
17	Fine sandstone	3.66
18	Silty mudstone	6.16
19	Fine sandstone	1.59
20	Coal seam	5
21	Silty mudstone	5

The first column denotes the serial number of each rock layer from top to bottom

gravity and mining deformation, and if these exceed the soil shear strength, the soil structure would be destroyed and generate cracks (Palchik 2003). We hypothesize that the soil mass is an isotropic and continuous half-space material, thus the normal pressure,  $\sigma$ , and the shearing strength,  $\tau_f$ , obey Coulomb's Law (Wu et al. 2010):

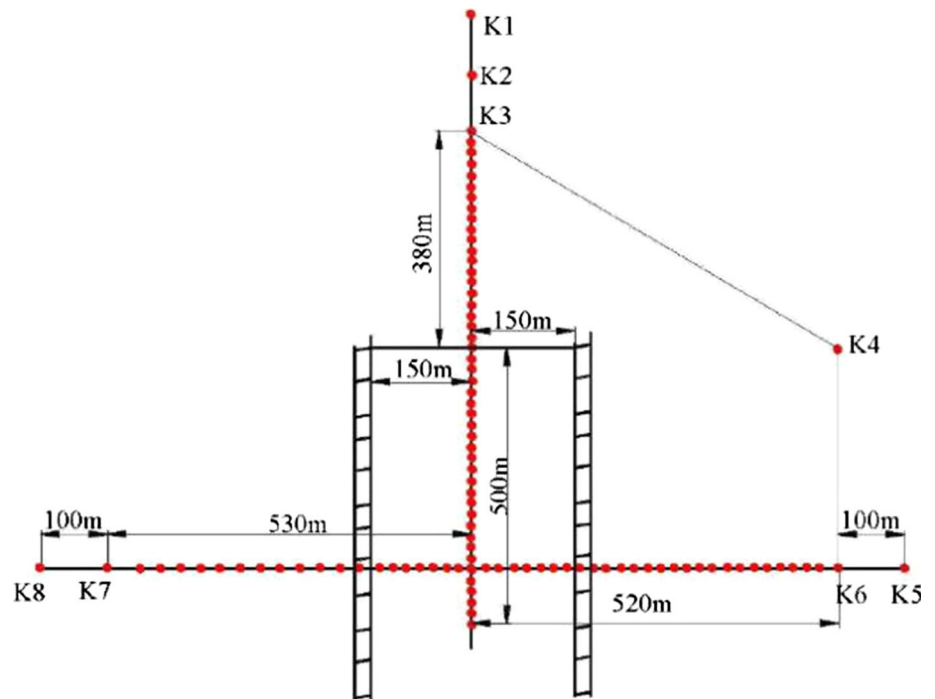
$$\tau_f = \sigma \tan \phi + c \quad (1)$$

where  $\tau_f$ ,  $\phi$ , and  $c$  denote shearing strength, internal friction angle, and cohesion of soils, respectively, and  $\sigma$  denotes the normal pressure on the shear plane.

From Eq. (1), we can see that the shear strength of the soil mass is related to its internal friction angle and cohesion, which differs as the soil physical properties changes. As there are significant differences in cohesion and internal friction angle between clay and aeolian sand, the unique development of cracks in the study area may be tightly linked to the physical properties of the topsoil.

To further verify the hypothesis that the secondary development of ground cracks in the Ordos region is due to the special mechanical properties of surface aeolian sand, we selected two typical coal mines, Bulianta mines and Baodian mines, to conduct comparative analysis. The Bulianta mines are located in western China with topsoil

**Fig. 1** Distribution of observation points. The black rectangle in the middle indicates the 300 × 500 m working face; the 99 observation points and the eight control points, K1–K8, are shown in red (Hu et al. 2014)



composed of aeolian sand, while the Baodian mines are located in eastern China, and its surface layer includes silty soil, silty clay, and clay. Using the mechanical parameters of ground soil, the maximum development depth of ground cracks can be calculated (Wu et al. 2010). If the calculated maximum depth is less than the in situ measured depth in Bulianta mines, while that in Baodian mines is larger than the measured value, our hypothesis can be verified (see “Theoretical analysis based on soil mechanics” section).

## Results and discussion

### Second development of surface cracks

There were 55 fissures observed in the study area, in which the intact development processes of five cracks were successively recorded. As shown in Fig. 2, ground cracks were generated encircling the mined-out area in an oval shape. The five selected fissures were located near to the central line of the working face.

Unlike the in situ monitoring results obtained in eastern China, where ground cracks only undergo a unimodal cycle (Ni and Wang 2014; Yuan and Wu 2003), the cracks in the Bulianta mines show an unusual bimodal development cycle. As shown in Fig. 3, although the maximum width and formation time of the five cracks vary, they all go through a similar development process. As the working face moves forward, the cracks first undergo a rapid “expanding-closure” cycle, followed by another “expanding-

closure” cycle at a much slower speed. Moreover, the crack width in the first cycle has a peak width that is far larger than the second, approximately 1.4–3.8 times that of the latter.

### Theoretical interpretation of the secondary development ground cracks

#### *The perspective of strata control*

One possible cause of the secondary development ground cracks is the two groups of hard rock layers called key strata (Li et al. 2017) above the coal seam, which successively break in the excavation process. As the hard rock layers play a key role in strata movement, each time a key stratum fractures, large tensions arise in the ground soil and opening surface cracks. Therefore, the secondary development ground cracks may be attributed to the breakage of two key strata (Fig. 4). However, this logic fails to explain the first crack closure, because our field measurement data show that at the first closure, the cracks are under a state of tension (Fig. 5). This should only lead to crack expansion and not closure. To verify this conclusion, we made a further analysis of the in situ ground subsidence data.

We selected one ground fissure in the Bulianta mines, fissure F1, and its neighboring point, B42, as an example for analyzing the relationship between ground settlement surface crack developments (Fig. 2). As shown in Fig. 5, when fissure F1 first closed, the subsidence value for point B42 reached half of its maximum subsidence. Furthermore,

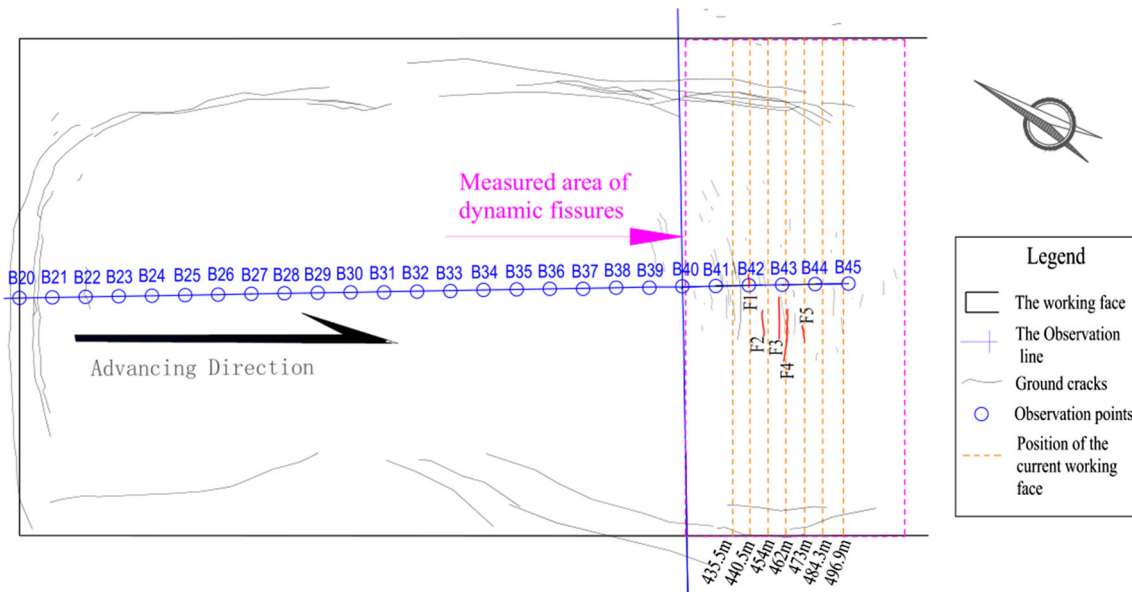


**Fig. 2** Distribution of ground cracks. Five fissures marked in red, F1–F5, were successively recorded (adapted from Li et al. 2017). The center of the small blue circles marked with blue numbers represents

the location of observation points, and the neighboring observation points are about 20 m distant from each other. Observation point B42 is only 0.2 m in distance from fissure F1

**Fig. 3** Bimodal development of ground cracks. **a–e** Correspond to fissures F1–F5, respectively. The working face had advanced to 431, 440.5, 462, 473, and 484.3 m when surface fissures F1–F5 were, respectively, first observed. Adapted from Hu et al. (2014)

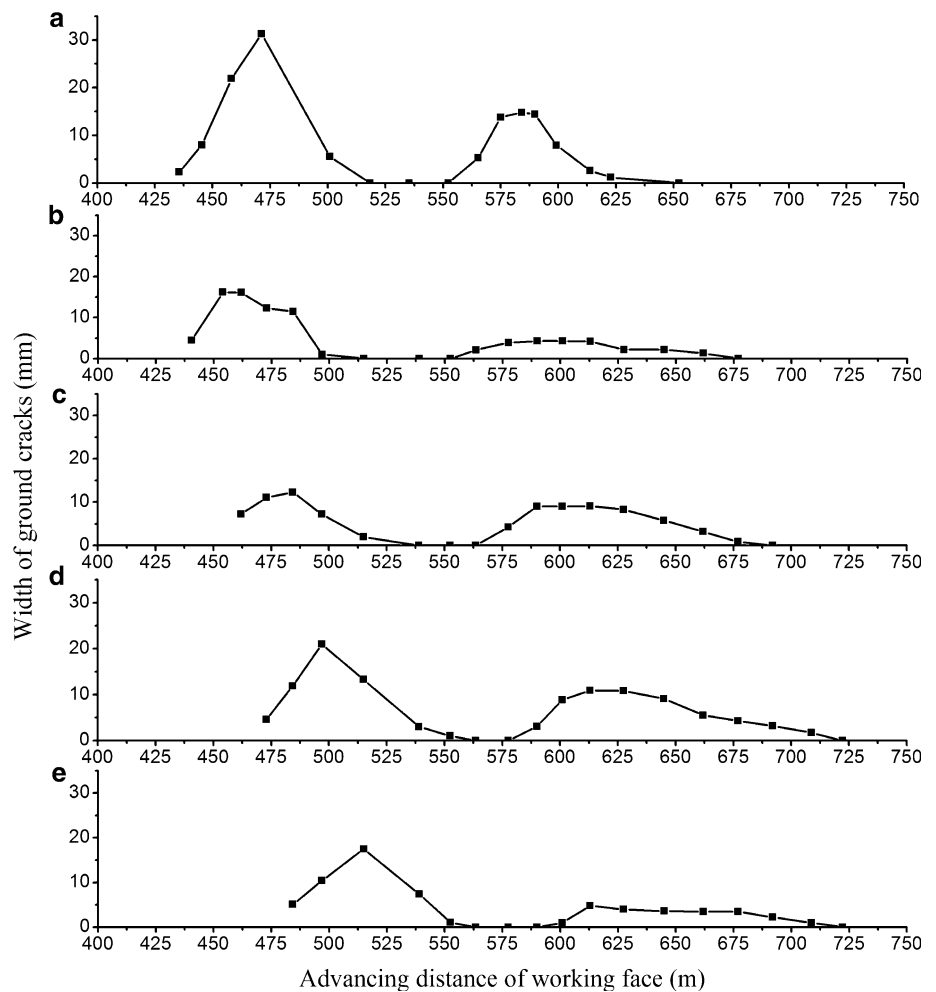
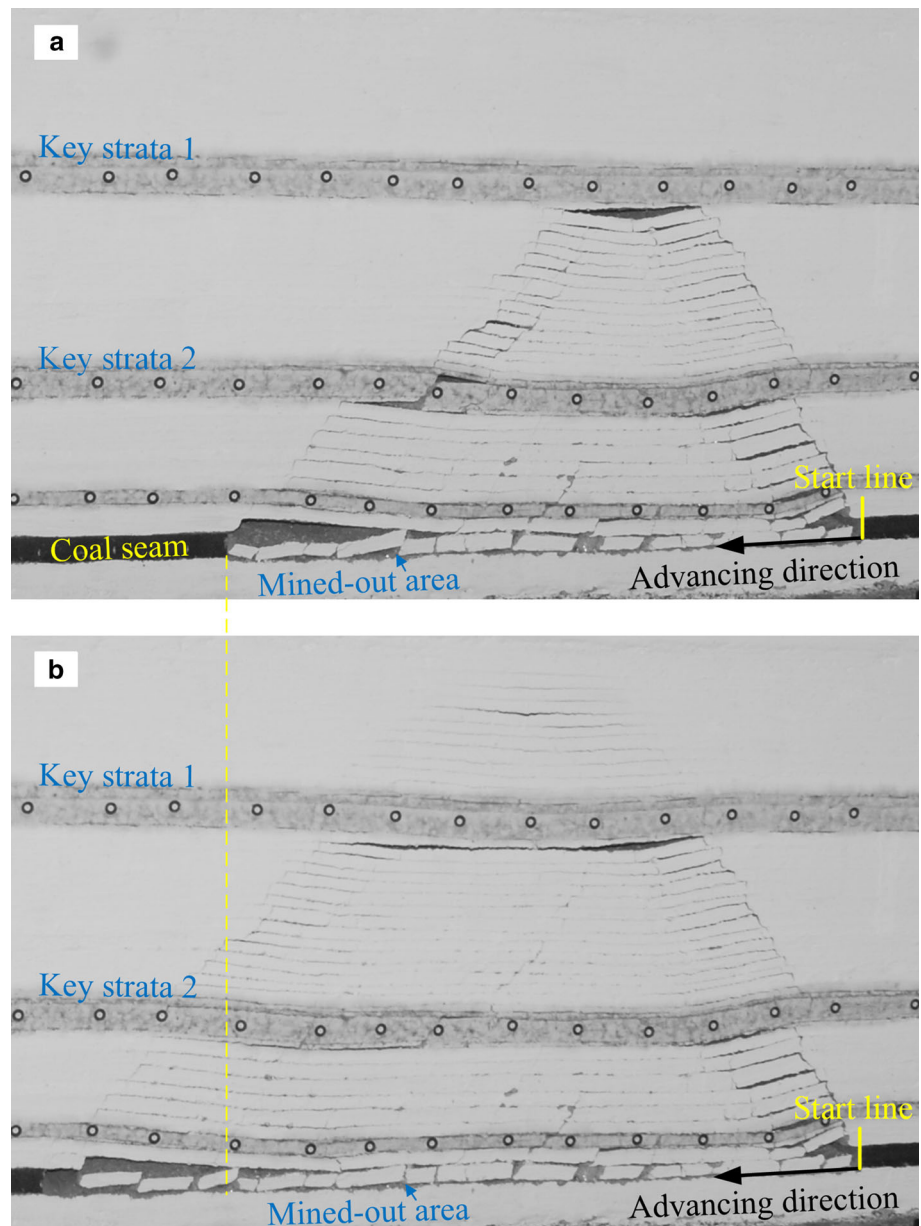


**Fig. 4** Simulated fracture of two key strata using a physical model composed of sand, plaster, and calcium carbonate. **a** The fracture of key stratum 2 and **b** the fracture of key stratum 1. The rationale of physical model can be referred to Xu et al. 2017, and the detailed information of the physical model shown in Fig. 4 can be referred to Li et al. 2017



the settling speed for point B42 peaked at this time. Because all ground points went through an almost same development process of first increasing and then decreasing in the whole mining process, when the subsidence speed of point B42 reached the maximum, it also meant that the subsidence speed of its neighboring points, B41 and B43, had not reached the peak (Fig. 2). This suggested point B42 subsided faster than all other neighboring points at this moment. Therefore, fissure F1 was still located in tensile zone when it went through the first closure.

In addition, though we successfully observed that the two key strata fractured one after another from the physical model (Fig. 4), the ground cracks on the model only underwent one “expansion-closure” cycle, and this can be

further verified by the experiment conducted by Xu et al. 2017.

#### *Theoretical analysis based on soil mechanics*

In this work, another possible cause is hypothesized based on soil mechanics. Namely, the initial surface crack closure may be attributed to shear failure due to the internal gravity of the soil mass (Terzaghi 1943; Taylor 1948). If the soil mass is regarded as an elastic half-space material, the top and bottom of a micro-body of soils of depth  $H$  have an internal gravity stress:  $\sigma_1 = \gamma H$ , where  $\sigma_1$  denotes vertical micro-body stress, and  $\gamma$  denotes the average bulk density of the soil mass. The micro-body is also influenced by the

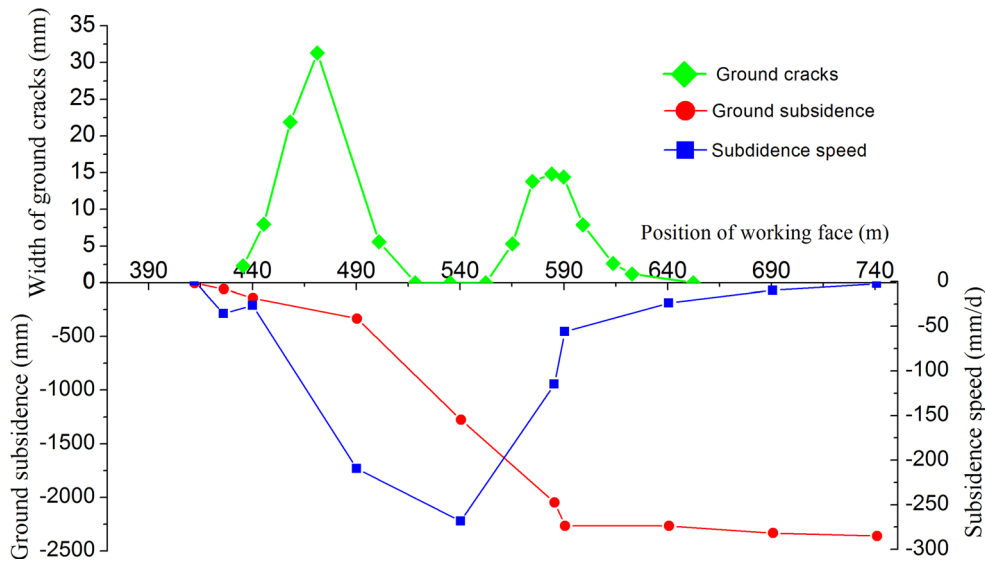


**Fig. 5** Relationship between ground subsidence and development of surface cracks. The subsidence speed is the ground subsidence occurred divided by the time elapsed. In an intact development cycle of ground cracks, the subsidence speed of an arbitrary point on the ground firstly increases and then decreases, and it reaches the

maximum at the first closure of ground cracks. The thickness of the coal seam is 5 m, and the maximum ground subsidence is about 2.5 m, thus the rate of settlement is about 0.50 (Xu et al. 2017). The working face advances continuously for 24 h a day, and the advancing speed is 12 m/day

lateral stress:  $\sigma_2 = \sigma_3 = \zeta\gamma H$ , where  $\zeta$  is the static lateral pressure coefficient.

As the micro-body is small enough, its self-gravity can be ignored. Furthermore, because the four sides of the micro-body bear equal stress, there is no shear strain and shear stress on these four sides. Therefore,  $\sigma_2$  and  $\sigma_3$  are the maximum and minimum principal stresses, respectively. According to static mechanics, the normal stress and shear stress of an arbitrary face can be calculated as:

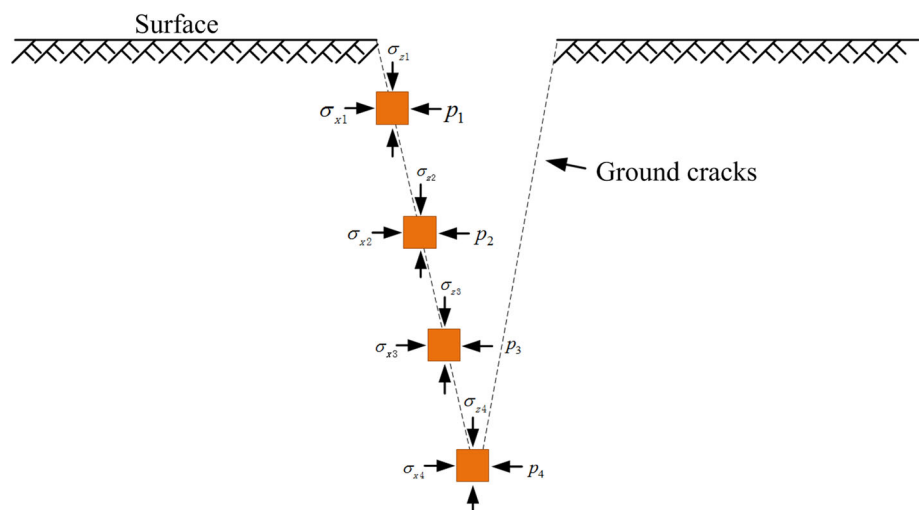
$$\sigma = \frac{\sigma_1 + \sigma_3}{2} + \frac{\sigma_1 - \sigma_3}{2} \cos 2\alpha \tag{2}$$

$$\tau = \frac{\sigma_1 - \sigma_3}{2} \sin 2\alpha \tag{3}$$

where  $\alpha$  is the angle between the target plane and horizontal plane. The relationship between normal stress and shear stress can be expressed as Mohr's circle.

After the ground cracks are generated, the minimum lateral stress of the soils near the fissures decreases to zero, and the previous mechanical equilibrium is destroyed. When the crack depth is small, the soil mass on the two sides of cracks does not cave in, due to soil cohesion. However, as surface cracks develop deeper, the principal stress  $\sigma_1$  increases gradually, and plastic flow deformation may occur in the soils and cause the soil mass to cave and fill the cracks, leading to the first ground crack closure (Fig. 6).

**Fig. 6** Stress analysis of a micro-body in cracked soils



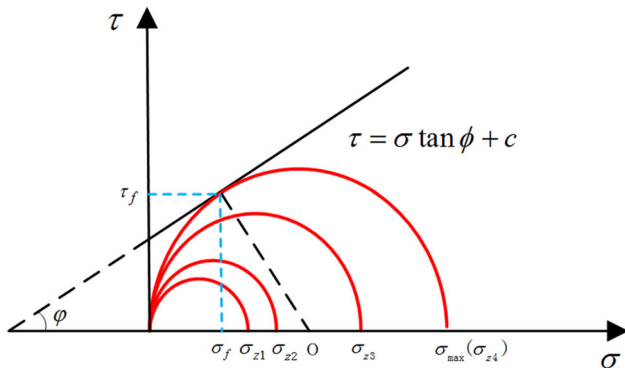


**Fig. 7** Shear failure analysis of soils surrounding ground cracks

The black solid line shown in Fig. 7 is called Mohr envelope; a state of limit equilibrium forms when the Mohr circle is tangent to the Mohr envelope. Soil failure occurs if the Mohr circle intersects the Mohr envelope. Because the maximum principal stress  $\sigma_{max} = \gamma H_{max}$ , we can obtain the maximum depth  $H_{max}$  using Eqs. (1)–(3):

$$H_{max} = \frac{2c \cdot (1 - \sin \phi)}{\gamma \cdot \cos \phi} = \frac{2c}{\gamma} \tan \left( 45^\circ + \frac{\phi}{2} \right) \tag{4}$$

If the depth of the surface cracks exceeds, the soil mass on the crack sides would cave and fill the fissures, even though they may be still in a state of tension. Therefore, the first closure of surface cracks is more likely induced by soil gravity failure, rather than compressive deformation.

After the first closure, the cracks are still located at the tensile zone, and the closed surface cracks will reopen after

a transient equilibrium. Due to the gradually decreasing tensile deformation of the ground during this process, and the prior “expanding-closure” cycle, the width of the reopened surface cracks decreases. In the end, with ground deformation turning from tensile to compressive, the surface cracks will undergo the second closure and reach a stable state.

**Numerical calculation and results**

We selected two coal mines, the Bulianta and Baodian mines, as a comparison to analyze the influence of soil properties on the development mechanisms for surface cracks. The Bulianta mines are located in northwestern China and are covered by 17-m-thick aeolian sand, while the Baodian mines are located in eastern China, of which the surface layer is primarily composed of 110-m-thick clay (Fig. 8).

The mechanical parameters for aeolian sand in the Bulianta mines (Bi et al. 2014; Song 2011) and those for soil mass in Baodian mines (Ni and Wang 2014) were compiled and are listed in Table 2.

From Table 2, it is clear that the surface soils in the Bulianta mines apparently have smaller cohesions and larger frictional angles. Substituting these parameters into Eq. (4), we can obtain the maximum crack depths where soil masses are still able to remain stable, namely 0.88 m in the Bulianta mines and 5.62 m in the Baodian mines. These two mines have similar mining conditions (Hu et al. 2014;

**Fig. 8** a Surface layer of the Bulianta mines and b ground cracks at the Baodian mines

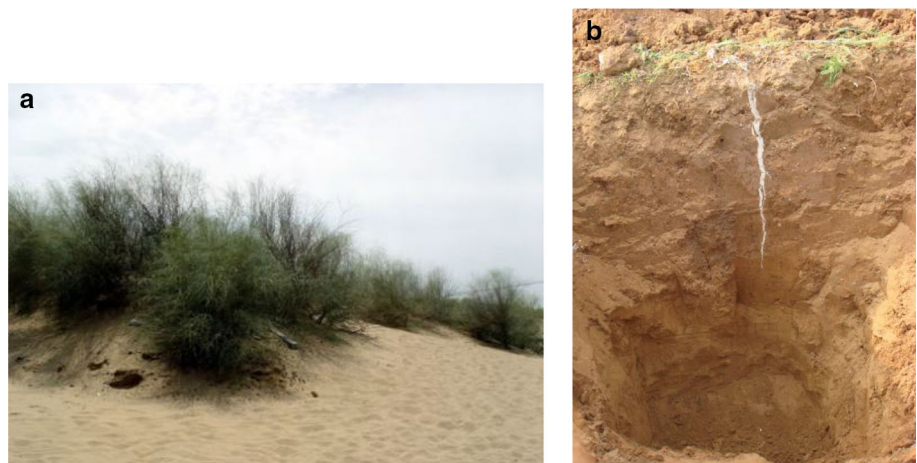


**Table 2** Mechanical parameters of surface soils in the Bulianta and Baodian mines

Name	Soil type	Bulk density (kN/m <sup>3</sup> )	Cohesion (kPa)	Fictional angle (°)
Bulianta mines	Aeolian sand	16.5	3.65	36.45
Baodian mines	Silty soil	18.7	23	24.8
	Silty clay	18.9	43	10.6
	Clay	18.1	57	10.1

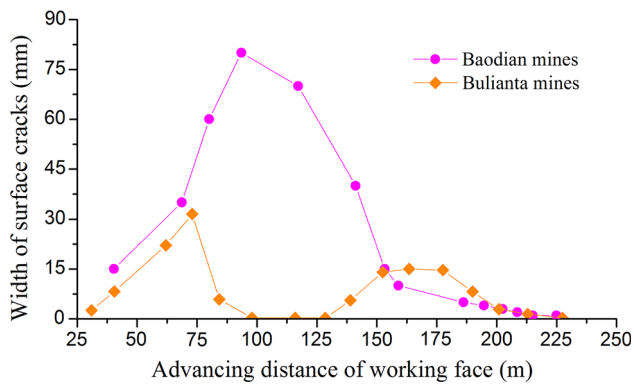


**Fig. 9** Development process of typical ground cracks in the Baodian and Bulianta mines

Ni and Wang 2014), while surface cracks develop differently. The cracks in the Baodian mines only go through one “expanding-closure” cycle, while those in the Bulianta mines undergo two “expanding-closure” cycles (Fig. 9). In both mines, the working face advances approximately 200 m in a full development cycle, from the first opening to the last closure.

By digging out the cracks that are filled with mixture of plaster and water, we can observe the shape of ground cracks clearly and measure their accurate development depth (Fig. 8b). There are totally four surface cracks in Baodian mines (Ni and Wang 2014) and 40 ground cracks in Bulianta mines randomly selected to measure the development depth (Table 3). As the depth of ground cracks is measured in several consecutive days, and during this period, some cracks may have started to close, thus the measured depth is equal to or smaller than the maximum development depth of each crack.

According to in situ data in Table 3, the maximum surface crack depth in the Baodian mines is 2.97 m, less than 5.62 m, thus surface cracks remain stable even if developing to the maximum depth. In contrast, the measured maximum crack depth in the Bulianta mines is 1.12 m, close to the theoretically calculated value, 0.88 m; therefore, soil around the cracks may lose stability and cause fissures to close after reaching the depth limit. Subsequently, the surface cracks remain in a state of tension, causing the cracks to reopen, influenced by residual horizontal deformation, but the maximum width opening is far smaller than the original opening crack width.

## Conclusions

In the Ordos region, China, ground cracks induced by underground coal excavation demonstrate an unusual secondary development. In particular, surface dynamic cracks undergo two “expanding-closure” cycles. Moreover, when

**Table 3** Depth of cracks randomly selected in Baodian and Bulianta mines. *BD-01* and *BLT-01* denotes the No. 1 ground crack in Baodian and Bulianta mines, respectively

No.	Depth (mm)
<i>BD-01</i>	2970
<i>BD-02</i>	2830
<i>BD-03</i>	2650
<i>BD-04</i>	800
<i>BLT-01</i>	710.3
<i>BLT-02</i>	152.2
<i>BLT-03</i>	1092.4
<i>BLT-04</i>	658.6
<i>BLT-05</i>	356.7
<i>BLT-06</i>	1120.8
<i>BLT-07</i>	432.6
<i>BLT-08</i>	43.2
<i>BLT-09</i>	343.2
<i>BLT-10</i>	822.6
<i>BLT-11</i>	145.6
<i>BLT-12</i>	158.3
<i>BLT-13</i>	68.4
<i>BLT-14</i>	393.1
<i>BLT-15</i>	51.2
<i>BLT-16</i>	52.3
<i>BLT-17</i>	255.3
<i>BLT-18</i>	138.3
<i>BLT-19</i>	1144.2
<i>BLT-20</i>	205.8
<i>BLT-21</i>	167.5
<i>BLT-22</i>	286.9
<i>BLT-23</i>	487.6
<i>BLT-24</i>	275.6
<i>BLT-25</i>	114.3
<i>BLT-26</i>	401.3
<i>BLT-27</i>	623.4
<i>BLT-28</i>	597.8
<i>BLT-29</i>	585.3
<i>BLT-30</i>	475.2
<i>BLT-31</i>	496.4
<i>BLT-32</i>	445.7
<i>BLT-33</i>	356.4
<i>BLT-34</i>	845.6
<i>BLT-35</i>	72.5
<i>BLT-36</i>	273.4
<i>BLT-37</i>	553.4
<i>BLT-38</i>	502.5
<i>BLT-39</i>	702.3
<i>BLT-40</i>	560.3

the ground cracks evolve through the first closure, the cracks remain in a tensile zone. Therefore, this phenomenon cannot be reasonably interpreted as due to strata failure. Through a comparison of ground dynamic cracks in

the Baodian mines, China, we propose a novel explanation for this phenomenon from the perspective of soil mechanics. Because the surface aeolian layer covering the Ordos area has very weak cohesion, when cracks develop to certain depth, soil failure occurs and fills the cracks. This mechanism is the cause of secondary surface crack development in the Bulianta mines. The results were well in agreement with our field measurement data. However, as field surveying work is time and labor consuming, currently we only obtained a small amount of in situ data in Bulianta mines, more data in the Ordos region is still required to further verify the conclusion.

**Acknowledgements** This work was supported by the Natural Science Foundation of China and Shenhua Group Co., Ltd (Grant No. U1361203). The authors would like to thank the editor and reviewers for their contributions to the paper.

### References

- Bi YL, Zou H, Zhu CHW (2014) Dynamic monitoring of soil bulk density and infiltration rate during coal mining in sandy land with different vegetation. *Int J Coal Sci Technol* 1(2):198–206
- Dunrud CR, Osterwald FW (1980) Effects of coal mine subsidence in the Sheridan, Wyoming, area. Center for Integrated Data Analytics Wisconsin Science Center, Middleton
- Hu ZHQ, Wang XJ, He AM (2014) Distribution characteristic and development rules of ground fissures due to coal mining in windy and sandy region. *J Chin Coal Soc* 1:11–18 (in Chinese)
- Li L, Wu K, Hu ZHQ, Xu YK, Zhou DW (2017) Analysis of developmental features and causes of the ground cracks induced by oversized working face mining in an aeolian sand area. *Environ Earth Sci* 76(3):135
- Ni XH, Wang FQ (2014) Technical study and practice of thick coal mining under watercourse in Technical study and practice of thick coal mining under watercourse in Yanzhou mining area. China University of Mining and Technology Press, Xuzhou, p 202 (in Chinese)
- Palchik V (2003) Formation of fractured zones in overburden due to longwall mining. *Environ Geol* 44(1):28–38
- Prakash A, Kumar A, Singh KB (2014) Dynamic subsidence characteristics in Jharia Coalfield, India. *Geotech Geol Eng* 32(3):627–635
- Singh TN, Singh DP (1992) Prediction of instability of slopes in an opencast mine over old surface and underground workings. *Int J Surf Min Reclam Environ* 6(2):81–89
- Sirdesai NN, Singh R, Singh TN, Ranjith PG (2015) Numerical and experimental study of strata behavior and land subsidence in an underground coal gasification project. *Proc IAHS* 372:455–462
- Song YX (2011) Test study on the mechanical property of the aeolian sand and the bearing capacity of the aeolian sand ground of Mu Us Desert. Chang’an University, Xi’an (in Chinese)
- Taylor DW (1948) *Fundamentals of soil mechanics*. LWW 66(2):161
- Terzaghi K (1943) *Theoretical soil mechanics*, vol 18. Wiley, New York
- Verma AK, Saini MS, Singh TN, Dutt A, Bajpai RK (2013) Effect of excavation stages on stress and pore pressure changes for an underground nuclear repository. *Arab J Geosci* 6:635–645
- Wang XJ (2014) Monitoring, evolution and self-healing characteristic of land damage due to high tension coal mining in windy and sandy area. China University of Mining and Technology, Beijing (in Chinese)
- Wu K, Li L, Ao JF, Hao G (2010) Discussion on limit development depth of cracks in surface soil mass caused by mining subsidence. *Coal Sci Technol* 38:108–111 (in Chinese)
- Xu YK, Wu K, Li L, Zhou DW, Hu ZHQ (2017) Ground cracks development and characteristics of strata movement under fast excavation: a case study at Bulianta coal mine, China. *Bull Eng Geol*. doi:10.1007/s10064-017-1047-y
- Yuan L, Wu K (2003) Technical study and practice of thick coal mining under watercourse in Theoretical study and technology practice of coal mining under Huaihe River embankment. China University of Mining and Technology Press, Xuzhou (in Chinese)